

# Universal physics of two neutrons with one flavored meson

Udit Raha,<sup>1,\*</sup> Yuki Kamiya,<sup>2,†</sup> Shung-Ichi Ando,<sup>3,‡</sup> and Tetsuo Hyodo<sup>2,§</sup>

<sup>1</sup>*Department of Physics, Indian Institute of Technology Guwahati, 781 039 Assam, India*

<sup>2</sup>*Yukawa Institute for Theoretical Physics, Kyoto University, Kyoto 606-8502, Japan*

<sup>3</sup>*Department of Information Communication and Display Engineering,  
Sunmoon University, Asan, Chungnam 31460, Korea*

(Dated: June 15, 2019)

We investigate the  $s$ -wave three-body system of two neutrons and one flavored meson with total spin-isospin  $J = 0, I = 3/2$ . The meson-neutron scattering length can become infinitely large in an unphysical region of the quark mass when extrapolated from strangeness to charm in the so-called zero coupling limit. Using a low-energy cluster effective field theory, we demonstrate that the Efimov effect is manifest in the three-body system when the meson-neutron scattering length is extrapolated to the unitary limit of the two-body interaction. We thereby discuss the consequence of universal physics in the physical  $K^-nn$  and  $D^0nn$  systems.

## I. INTRODUCTION

Few-body systems of an antikaon and nucleons are of great interest in the strangeness nuclear physics [1, 2]. The existence of the  $\Lambda(1405)$  resonance below the  $\bar{K}N$  threshold implies that the  $\bar{K}N$  interaction in the isospin  $I = 0$  channel is strongly attractive, with which the antikaon could be bound in nuclei [3, 4]. Recently, three-body  $\bar{K}NN$  systems have been a matter of intensive investigation based on rigorous few-body techniques [5–17]. To maximize the  $I = 0$  contribution of the  $\bar{K}N$  pair in the  $s$ -wave  $\bar{K}NN$  system, the state with the total spin  $J = 0$  and the isospin  $I = 1/2$  is mainly studied. It is agreed among several different groups that the  $J = 0$  system supports a quasi-bound state below the threshold, although the quantitative predictions are not yet well converged. There are some studies of the state with  $J = 1$  and  $I = 1/2$ , but the quasi-bound state is not found below the  $\Lambda^*N$  threshold in Refs. [14, 18], presumably because of the small fraction of the  $I = 0$  component of the  $\bar{K}N$  pair. In Ref. [12], it is shown that the  $J = 2$  and  $I = 3/2$  state is bound because of the  $p$ -wave  $\bar{K}N$  interaction that generates the  $\Sigma(1385)$  state.

Currently, nuclei with a heavy flavor (charm and bottom) meson is a subject matter drawing increasing attention [19]. This is triggered by the observation of many new heavy quarkonium-like hadronic states, called  $XYZ$ , above the open-charm or open-bottom thresholds [20–22]. Because the near-threshold states are often interpreted as *hadronic molecular states*, the existence of the  $XYZ$  states indicates that the heavy flavor meson could be a constituent in the formation of such exotic hadronic bound states. To assess the possible existence of the bound heavy mesons in nuclei, two-body  $DN$  interactions [23–28] and three-body quasi-bound systems [29, 30] involving  $D$  mesons have been

studied extensively. With a plethora of high-precision data currently available from a host of modern experimental facilities such as BaBar, Belle, CDF, D0, BES, CMS, LHCb, etc., similar investigations are also being extended to the open-bottom sector.

In general, the dynamics of a three-body problem reflects subtle details of two-body interactions. In some circumstances, gross properties of three-body systems can be assessed in terms of a few parameters which solely characterize the nature of two-body interactions. In fact, when the two-body scattering length  $a$  is much larger than the interaction range  $r_0$ , microscopic details of two-body interactions become irrelevant as a consequence of the low-energy *universality* [31, 32]. Universal physics can manifest themselves in sharply contrasting manner in the two- and three-body sectors. In the two-body sector, universal predictions are quite simple, manifested, e.g., as a shallow two-body bound state *dimer* for  $a > 0$  with the eigenenergy in the scaling limit given as  $E_{\text{dimer}} = -1/(2\mu_{\text{red}}a^2)$ , where  $\mu_{\text{red}}$  is the generic two-body reduced mass. However, universal predictions can become more complex in the three-body sector. The most striking phenomena in the three-body problem is the so-called *Efimov effect* [33], characterized by the emergence of infinitely many and arbitrary shallow geometrically spaced bound states with accumulation point at zero energy in  $s$ -wave three-body systems. In the context of hadron physics, the Efimov effect and low-energy universality have been discussed in the three-nucleon systems [34], the charmed meson systems [35], the three-pion systems [36], and the hyperon systems, such as the  $nn\Lambda$  system [37].

In this work we shed a new light on the meson-nucleus systems having a strange (charm) quark, from the viewpoint of the low-energy universality. We focus on the  $\bar{K}NN$  ( $DNN$ ) system with  $J = 0, I = 3/2$ , and  $I_3 = -3/2$ , or more specifically, the  $K^-nn$  ( $D^0nn$ ) system. In these systems, all the two-body interactions occur in the  $I = 1$  combinations. In comparison to other quantum numbers, the quantum numbers associated with the  $K^-nn$  ( $D^0nn$ ) channel are ideal to examine the Efimov effect due to the following reasons. First, the ab-

\* udit.raha@iitg.ernet.in

† yuki.kamiya@yukawa.kyoto-u.ac.jp

‡ sando@sunmoon.ac.kr

§ hyodo@yukawa.kyoto-u.ac.jp

sence of the Coulomb interaction guarantees that the low-energy behavior of this system is only governed by the two-body scattering lengths of the strong interaction. Second, the absence of any nearby coupled channels is also suitable for our purpose, otherwise the existence of such coupled channels is known to generally reduce the effective attraction in the three-body system [35, 36] diminishing the likely-hood of formation of Efimov bound states.

While the scattering length of the two-neutron system is much larger than the typical length scale of the strong interaction, we should note that the magnitude of the  $K^-n$  ( $D^0n$ ) scattering length is not large enough for the meson-neutron two-body system to become resonant. However, our analysis reveals that the meson-neutron scattering length is expected to reach the unitary (resonant) limit, through an extrapolation of the quark mass from strange to charm where the couplings to sub-threshold decay channels are neglected for simplicity. Consequently with such a *zero coupling limit* (ZCL) approximation, the otherwise complex meson-neutron scattering lengths turn out to be real valued. This obviously leads to a considerable simplification of the analysis of the three-body *Faddeev-like* system of integral equation from that of a more involved 'realistic' analysis with complications due to coupled multi-channel dynamics involving also hadrons other than the  $K^-$  ( $D^0$ ) meson and the neutron. Such an sophisticated approach is currently beyond the scope of our *naive* low-energy effective field theoretical (EFT) framework that we use in this work. Our primary objective in this paper is to present a rather qualitative analysis in the context of a simplistic EFT to illuminate certain aspects of remnant two- and three-body universal physics that may indicate possibilities of bound state (*dimer* and *trimer*) formation in physical systems such as  $K^-n$  ( $D^0n$ ) and  $K^-nn$  ( $D^0nn$ ).

This paper is organized as follows. In Sec. II, we study the two-body interaction of a flavored meson ( $K^-$  or  $D^0$ ) with a neutron in the  $I = 1$  state. We introduce a coupled-channel scattering model to perform the extrapolation from strangeness to charm. We evaluate the two-body scattering length in this extrapolation, together with the ZCL approximation with couplings to sub-threshold decay channels switched off. In Sec. III, we formulate a *pionless* cluster effective field theory which describes the low-energy properties and dynamics of a three-particle cluster state consisting of two neutrons and a flavored meson ( $K^-$  or  $D^0$ ). In particular, we consider a possible scenario where the  $s$ -wave meson-neutron scattering length is taken infinitely large, while the  $s$ -wave neutron-neutron scattering length is kept fixed at its physical value. We perform an asymptotic analysis of the system of three-body integral equations to examine the *limit cycle* renormalization group (RG) behavior and other associated features related to the Efimov effect. Our numerical results for the full non-asymptotic analysis of the integral equations with and without including a three-body interaction are then presented. The final sec-

tion is devoted to a summary of this work. Furthermore, based on our numerical results, a plausibility argument is presented at a qualitative level on the feasibility of  $K^-nn$  or  $D^0nn$  bound trimer formation. A discussion on certain numerical methodologies adopted in this work have been relegated to the appendices.

## II. TWO-BODY MESON-NEUTRON INTERACTION

### A. $K^-n$ system, $D^0n$ system, and the unitary limit

We first summarize the known properties of the meson-neutron interactions. In the  $\bar{K}N$  system, several experimental data constrain the meson-baryon scattering amplitude [1]. Among others, the recent measurement of the kaonic hydrogen by the SIDDHARTA collaboration [38, 39] gives a strong constraint on the low-energy  $\bar{K}N$  interaction, because the result is directly related to the  $K^-p$  scattering length through the improved Deser-type formula [40]. The analysis of the meson-baryon scattering with a complete *next-to-leading* order chiral SU(3) dynamics including the SIDDHARTA constraint [41, 42] determines the scattering lengths of the  $K^-n$  system as<sup>1</sup>

$$a_{0,K^-n} = -0.57_{-0.04}^{+0.21} - i0.72_{-0.26}^{+0.41} \text{ fm.} \quad (1)$$

The negative real part indicates that the  $K^-n$  interaction is attractive, but not strong enough to support a quasi-bound state. The imaginary part of the scattering length indicates possible decay into sub-threshold  $\pi\Sigma$  and  $\pi\Lambda$  channels.

The  $D^0n$  system is a counterpart of the  $K^-n$  system in the charm sector. In contrast to the strangeness sector, there is no experimental data for the  $D^0n$  scattering. Theoretically, the  $D^0n$  interaction has been studied by generalizing the established models in the strangeness sector [23–27] (see Ref. [19] for a recent review). Here we take an alternative strategy by using the experimental information of the  $\Sigma_c(2800)$  resonance. The mass and width of the neutral  $\Sigma_c^0(2800)$  state are given by the Particle Data Group as [22]

$$M_{\Sigma_c^0(2800)} = 2806_{-7}^{+5} \text{ MeV}, \quad \Gamma_{\Sigma_c^0(2800)} = 72_{-15}^{+22} \text{ MeV}, \quad (2)$$

which lies very close to the  $D^0n$  threshold at  $\sim 2803.8$  MeV. Although the spin and parity of  $\Sigma_c(2800)$  are not yet determined experimentally, by assuming  $J^P = 1/2^-$ , we can determine the strength of the  $s$ -wave interaction in the  $D^0n$  system. If the resonance pole of  $\Sigma_c(2800)$  is found to lie below the  $D^0n$  scattering threshold, then

<sup>1</sup> In this paper, the scattering length is defined as  $a_0 = -f(E=0)$  with the scattering amplitude  $f$ . The sign convention of the scattering length is opposite to that used in Refs. [41, 42].

the  $D^0n$  interaction is attractive enough to generate a quasi-bound state below the threshold. As will be demonstrated below, such a  $D^0n$  quasi-bound picture of the  $\Sigma_c(2800)$  resonance naturally arises in the SU(4) contact interaction model.

From these observations, we can draw the following conclusion regarding the scenario of the meson-neutron interaction. On the one hand, the  $K^-n$  system has a weakly attractive scattering length, as indicated by recent analysis in the strangeness sector. On the other hand, the  $D^0n$  system can support a quasi-bound state below the threshold, which is ostensibly identified with the observed  $\Sigma_c(2800)$  state. If we perform an extrapolation of the  $K^-n$  interaction to the  $D^0n$  interaction by changing the mass of the  $s$ -quark to that of the  $c$ -quark, we can expect the existence of an unphysical region of the quark mass between  $m_s$  and  $m_c$  where a very shallow bound/quasi-bound state is formed when the magnitude of the scattering length becomes infinitely large. This represents the universal region around the *unitary limit* of the meson-neutron interaction. The situation is analogous to the two-nucleon [34], the two-pion [36], and the  $\Lambda\Lambda$  [43] systems, where the unitary limit of the two-hadron scattering is achieved by the quark mass extrapolation into the unphysical region. In much the same way, in this work we plan to explore the universal physics in proximity to meson-neutron unitarity using unphysical quark masses between the strangeness and charm limits.

## B. Models of $\bar{K}N$ and $DN$ amplitudes

To demonstrate that the unitary limit is indeed realized through the extrapolation, we employ a contact interaction model with flavor symmetry. In the strangeness sector, the *Weinberg-Tomozawa model* approach in the chiral SU(3) dynamics successfully describes the  $\bar{K}N$  scattering [1, 44–46]. In the charm sector, the SU(4) generalization of this approach is developed in Ref. [24] in which the  $\Lambda_c(2595)$  resonance in the  $DN$  scattering is dynamically generated in the  $I = 0$  sector, analogously with  $\Lambda(1405)$  in the strangeness sector. Therefore, in this work we describe both  $\bar{K}N$  and  $DN$  systems within a common unified framework of a *dynamical coupled-channel model*.

The coupled-channel scattering amplitude  $T_{ij}(W)$  with the total energy  $W$  is given by the scattering equation

$$T(W) = [V^{-1}(W) - G(W)]^{-1}, \quad (3)$$

with the interaction kernel  $V(W)$ :

$$V_{ij}(W) = -\frac{C_{ij}}{f_i f_j} (2W - M_i - M_j) \sqrt{\frac{M_i + E_i}{2M_i}} \sqrt{\frac{M_j + E_j}{2M_j}}, \quad (4)$$

where  $C_{ij}$  is the coupling strength matrix specified below,  $M_i$  ( $E_i$ ) is the mass (energy) of the baryon in channel

$i$ , and for later convenience, we introduce the channel-dependent meson decay constant  $f_i$ . Using the dimensional regularization scheme, the loop function  $G(W)$  is given by

$$G_i(W; a_i) = \frac{2M_i}{16\pi^2} \left\{ a_i(\mu_{\text{reg}}) + \ln \frac{m_i M_i}{\mu_{\text{reg}}^2} + \frac{M_i^2 - m_i^2}{2W^2} \ln \frac{M_i^2}{m_i^2} \right. \\ \left. + \frac{\bar{q}_i}{W} [\ln(W^2 - (M_i^2 - m_i^2) + 2W\bar{q}_i) \right. \\ \left. + \ln(W^2 + (M_i^2 - m_i^2) + 2W\bar{q}_i) \right. \\ \left. - \ln(-W^2 + (M_i^2 - m_i^2) + 2W\bar{q}_i) \right. \\ \left. - \ln(-W^2 - (M_i^2 - m_i^2) + 2W\bar{q}_i) \right\}, \quad (5)$$

where  $m_i$  is the mass of the meson in channel  $i$ ,  $a_i(\mu_{\text{reg}})$  is the subtraction constant in channel  $i$  at the regularization scale  $\mu_{\text{reg}}$ , and the quantity  $\bar{q}_i = \sqrt{(W^2 - (M_i - m_i)^2)(W^2 - (M_i + m_i)^2)}/(2W)$  is the analytically continued three-momentum in the center-of-mass frame. In this model, the interaction strengths  $C_{ij}$  are basically determined by the flavor symmetry. The free parameters in the model are the subtraction constants  $a_i(\mu_{\text{reg}})$  at the regularization scale  $\mu_{\text{reg}}$ . In this convention, the (diagonal) scattering length  $a_{0,i}$  in channel  $i$  is given by

$$a_{0,i} = \frac{M_i}{4\pi(M_i + m_i)} T_{ii}(M_i + m_i). \quad (6)$$

Now we consider the model space of the scattering. Because we are interested in the energy region near the  $\bar{K}N/DN$  threshold, the higher energy channels (such as  $\eta\Sigma/\eta\Sigma_c$  and  $K\Xi/K\Xi_c$ ) are not very relevant to our analysis which we exclude. However, we only include the channels lower than the  $\bar{K}N$  and  $DN$  thresholds, respectively, namely,

$$K^-n, \quad \pi^-\Lambda, \quad \pi^0\Sigma^-, \quad \pi^-\Sigma^0 \quad (7)$$

in the strangeness sector, and the corresponding open channels in the charm sector:

$$D^0n, \quad \pi^-\Lambda_c^+, \quad \pi^0\Sigma_c^0, \quad \pi^-\Sigma_c^+. \quad (8)$$

The coupling matrix for these channels takes on the form

$$C = \begin{pmatrix} 1 & -\sqrt{\frac{3}{2}}\kappa & -\sqrt{\frac{1}{2}}\kappa & \sqrt{\frac{1}{2}}\kappa \\ & 0 & 0 & 0 \\ & & 0 & -2 \\ & & & 0 \end{pmatrix} \quad (9)$$

where the suppression factor  $\kappa$  is introduced for the heavy flavor exchange processes. The masses of hadrons relevant for these channels are taken from the central values by the Particle Data Group (PDG) [22] and summarized in Table I. We use the physical meson decay constants  $f_\pi = 92.4$  MeV and  $f_K = 109.0$  MeV, and the decay constant of the  $D$  meson is also chosen to be  $f_D = 92.4$  MeV, following Ref. [24].

TABLE I. Masses of hadrons.

Hadron	$K^-$	$\pi^-$	$\pi^0$	$n$	$\Lambda$	$\Sigma^-$	$\Sigma^0$	$D^0$	$\Lambda_c^+$	$\Sigma_c^0$	$\Sigma_c^+$
Mass [MeV]	493.677	139.57018	134.9766	939.565379	1115.683	1197.449	1192.642	1864.3	2286.46	2453.75	2452.9

TABLE II. Subtraction constants  $a_i(\mu_{\text{reg}})$  at the regularization scale  $\mu_{\text{reg}} = 1000$  MeV.

	$a_1$	$a_2$	$a_3$	$a_4$
Strangeness	-1.283	0.238	-0.714	-0.714
Charm	-1.663	-2.060	-2.060	-2.060

The remaining parameters are the subtraction constant  $a_i$  in each channel and the suppression factor  $\kappa$  in the coupling strength Eq. (9). To determine these parameters in the strangeness sector, it is essential to take into account the SIDDHARTA data of the kaonic hydrogen [38, 39]. The data allows a direct extraction of the  $K^-p$  scattering length as related through the improved Deser-type formula [40] and provides a strong constraint on the low-energy  $\bar{K}N$  interaction [41, 42]. In Ref. [42], a simplified model is constructed with the Weinberg-Tomozawa interaction ( $\kappa = 1$ ) in the model space of Eq. (7), but reasonably well reproducing the full next-to-leading order amplitude constrained by the SIDDHARTA data. Explicit values of the subtraction constants are summarized in the ‘‘Strangeness’’ row of Table II. The scattering length of the  $K^-n$  system is obtained as

$$a_{0,K^-n} = -0.135 - i0.410 \text{ fm.} \quad (10)$$

The value slightly deviates from the full result in Eq. (1), because of the simplified assumptions of this scattering model.

In the charm sector, the subtraction constants are determined in Ref. [24] by the argument of ‘‘natural size’’ [46, 47] with a slight modification of the constant associated with the  $DN$  channel necessary to reproduce the observed  $\Lambda_c^+(2595)$  resonance in the  $I = 0$  channel amplitude. Likewise, we essentially follow the same strategy in the present case with all  $I = 1$  two-body subsystems; the subtraction constants in channels 2-4 (i.e.,  $\pi^- \Lambda_c^+$ ,  $\pi^0 \Sigma_c^0$  and  $\pi^- \Sigma_c^+$ ) are given by the natural size, and the subtraction constant in channel 1 (i.e.,  $D^0n$ ) is used to reproduce the  $\Sigma_c(2800)$  state near the  $D^0n$  threshold. We also tune the value of  $\kappa$  to control the width of the resonance. By choosing the subtraction constants shown in Table II with  $\kappa = 0.453$ , we dynamically generate a resonance pole corresponding to the  $\Sigma_c(2800)$  state at

$$M = 2800 \text{ MeV}, \quad \Gamma = 72 \text{ MeV.} \quad (11)$$

In this model, the  $D^0n$  scattering length is found to be

$$a_{0,D^0n} = 0.764 - i0.615 \text{ fm.} \quad (12)$$

The positive real part is in accordance with the existence of the quasi-bound state  $\Sigma_c(2800)$  below the threshold. The origin of the  $I = 1$  quasi-bound state can be understood in the following argument. Because of the SU(4) symmetry, the interaction of the  $D^0n$  channel has the same sign with that of the  $K^-n$  channel, and the strength at the threshold is enhanced by the ratio  $m_D/m_K$ . Thus, we can expect a stronger attractive interaction in the  $D^0n$  channel. Moreover, the heavier reduced mass of the  $DN$  system leads to suppression of the kinetic energy, a crucial expedient in the formation of a bound state.

### C. Flavor extrapolation and zero coupling limit

We now introduce a parameter  $0 \leq x \leq 1$  which controls the extrapolation from strangeness to charm. Assuming linear relationship among the following model parameters, we linearly vary each as a function of  $x$ ;

$$m_i(x) = m_i^s(1-x) + m_i^c x, \quad (13)$$

$$M_i(x) = M_i^s(1-x) + M_i^c x, \quad (14)$$

$$a_i(x) = a_i^s(1-x) + a_i^c x, \quad (15)$$

$$f_i(x) = f_i^s(1-x) + f_i^c x, \quad (16)$$

$$\kappa(x) = \kappa^s(1-x) + \kappa^c x, \quad (17)$$

for the respective channels,  $i = 1, \dots, 4$ . Namely,  $x = 0$  ( $x = 1$ ) corresponds to the physical point of the model in the strangeness (charm) sector, while all other intermediate values of  $x$  represent the model in the unphysical domain. Thus, for instance in the  $i = 1$  channel, by varying  $x$  from 0 to 1, we can perform a linear extrapolation from the  $K^-n$  to the  $D^0n$  scattering sectors.

Now we study the behavior of the complex scattering length in the coupled-channel contact interaction model. The real and imaginary parts of the meson-neutron scattering length as functions of  $x$  are shown in Fig. 1. The scattering length varies continuously from  $a_{0,K^-n}$  to  $a_{0,D^0n}$  along with  $x$ . It is not immediately clear from this figure how to decipher the remnant of the universal features of meson-neutron unitarity in any straightforward manner due to effects of the sub-threshold decay channels. We note that in the present scenario, the S-matrix pole corresponding to the quasi-bound state of the  $D^0n$  system moves to the higher positive energy region as we decrease  $x$  from 1, eventually going far above the  $K^-n$  threshold at  $x = 0$  without yielding a bound  $K^-n$  state. The pole trajectory of the scattering amplitude is shown in Fig. 2. Note that the pole is on the Riemann sheet with physical momentum with respect to channel 1

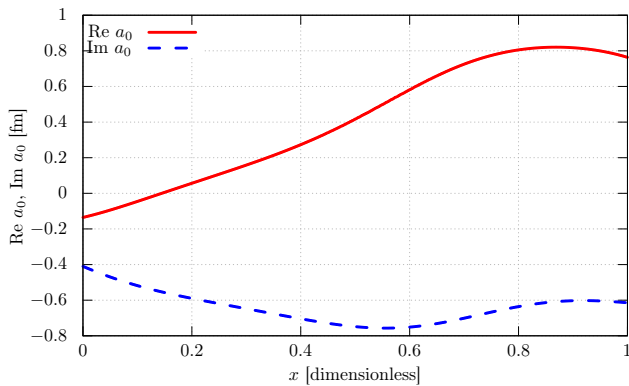


FIG. 1. Complex meson-neutron scattering length in the coupled-channel contact interaction model as a function of the extrapolation parameter  $x$ . Solid (dashed) line represents the real (imaginary) part.

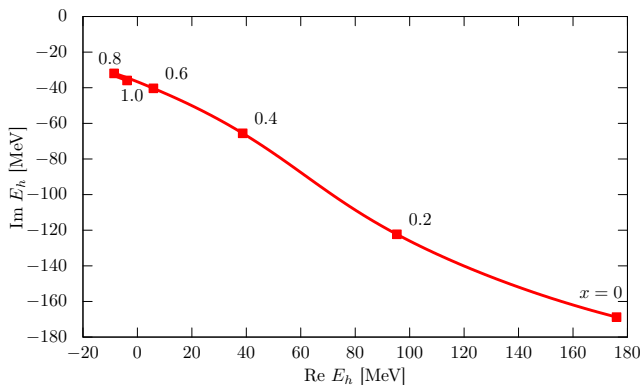


FIG. 2. Trajectory of the pole of the scattering amplitude in the coupled-channel contact interaction model. The energy is measured with respect to the threshold of the channel 1.

and unphysical momenta in regard to the others.<sup>2</sup> Thus, the pole directly influences the physical spectrum when  $\text{Re } E_h < 0$  (as in the charm sector  $x = 1$ ), being the most adjacent Riemann sheet to the physical real axis, while its effect is less significant when  $\text{Re } E_h > 0$  (as in the strangeness sector  $x = 0$ ), with the proximity of the pole position somewhat far away from the physical axis.

To elucidate a possible scenario to access the unitary limit of the meson-neutron interaction, we consider a zero coupling limit (ZCL) model in which the channel cou-

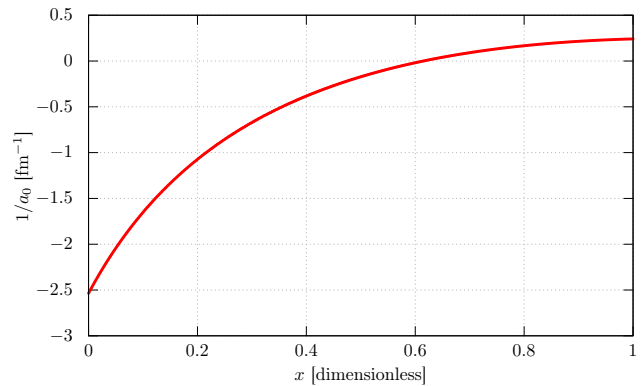


FIG. 3. Meson-neutron inverse scattering length in the absence of the decay channels in the zero coupling limit as a function of the extrapolation parameter  $x$ .

plings are switched off [48–50], i.e.,

$$C_{1i} = C_{i1} = 0 \quad \text{for } i = 2, 3, 4. \quad (18)$$

With this approximation, the coupled-channel problem reduces to a single-channel scattering of the  $K^-n/D^0n$  system. The  $K^-n$  system is again found to have no bound state, while the previous quasi-bound state in the  $D^0n$  channel now becomes a real bound state with invariant mass of  $W \sim 2802$  MeV. Correspondingly, the scattering length is real and negative (positive) in the  $K^-n$  ( $D^0n$ ) channel:

$$a_{0,K^-n}^{\text{ZCL}} = -0.394 \text{ fm}, \quad a_{0,D^0n}^{\text{ZCL}} = 4.141 \text{ fm}. \quad (19)$$

The above numerical values of the scattering lengths in the ZCL model strongly suggest that the meson-neutron interactions to become resonant somewhere in the intermediate unphysical region ( $0 < x < 1$ ). In Fig. 3, we display the result for the inverse scattering length  $1/a_0(x)$ , expressed as a function of the extrapolation parameter  $x$ . We indeed find that the unitary limit ( $1/a_0 = 0$ ) is achieved at  $x \sim 0.615$ . At this point, the extrapolated mass of the flavored meson in the channel 1 is

$$m_1(0.615) = 1336.61 \text{ MeV}. \quad (20)$$

The corresponding behavior of the pole trajectory in the zero coupling limit is shown in Fig. 4. The *real* bound state pole at  $x = 1$  that lie on the *physical (first) Riemann sheet* turns into a *virtual state* pole at the unitary limit moving onto the *unphysical Riemann sheet*. As we further decrease  $x$ , the virtual state pole eventually meets with a second virtual state pole on the unphysical sheet and then acquires a finite width [51]. In particular, at  $x = 0$ , the virtual state pole remains below the threshold with finite imaginary part, but still on the unphysical sheet.

<sup>2</sup> In an  $n$ -channel problem, the scattering amplitude is defined on a  $2^n$ -sheeted Riemann surface in the complex energy plane with momentum  $p_i$  and  $-p_i$  in channel  $i$  corresponding to the same energy. The Riemann sheet is specified by choosing either the physical momentum ( $\text{Im } p_i > 0$ , first sheet) or the unphysical momentum ( $\text{Im } p_i < 0$ , unphysical sheet) for each channel  $i$ . The most adjacent Riemann sheet to the real scattering axis is obtained by choosing the physical momentum in the open channels and unphysical momentum in the closed channels.

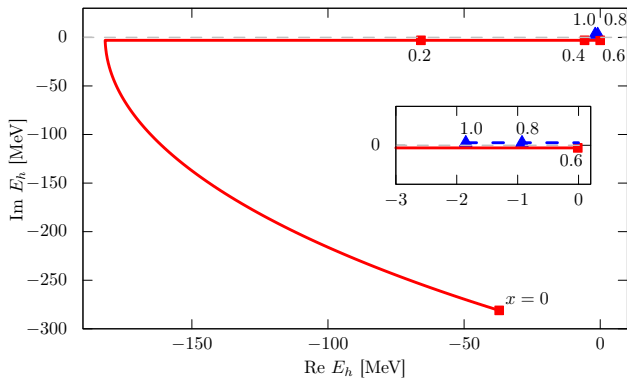


FIG. 4. Trajectory of the pole of the scattering amplitude in the zero coupling limit. The energy is measured with respect to the threshold of the channel 1. Dashed (solid) line represents the pole in the physical (unphysical) Riemann sheet.

#### D. Universality in the two-body sub-system

It is instructive to take another look at the above results from the viewpoint of the two-body universality. When the magnitude of the scattering length  $|a_0|$  becomes large and approaches the unitary limit, universality suggests that there exists a two-body meson-neutron eigenstate with the eigenmomentum

$$k_a = i/a_0, \quad (21)$$

up to corrections suppressed by effective range terms. This relation holds even for a complex  $a_0$ . Thus, if we calculate the eigenmomentum  $k_h$ , that correspond to the pole position of the scattering amplitude in the system with a large scattering length, the true eigenvalue  $k_h$  can be well approximated by  $k_a$  in the two-body universal region. The deviation of  $k_h$  from  $k_a$  thus serves as a measure of the violation of the universality.

We show in Fig. 5 the deviation of the eigenmomentum from the universal prediction  $|k_h - k_a|$  as a function of  $x$ . Although there is a large deviation in the strangeness sector ( $x = 0$ ), the universal value  $k_a$  around  $x \sim 0.8$ , including the  $D^0n$  system at  $x = 1$ , gives a reasonable prediction of the true eigenvalue  $k_h$ . This shows the relevance of the low-energy universality in the meson-neutron system around the charm quark sector.

The situation becomes much more conspicuously in the ZCL model. As shown in Fig. 6, we see a quite good agreement of  $k_h$  with  $k_a$ , not only in the vicinity of the unitary limit ( $x \sim 0.615$ ) but also in the entire region of  $x \gtrsim 0.3$ . We should note that the eigenstate in the unbound region ( $x \lesssim 0.615$ ) corresponds to a virtual state ( $a_0 < 0$ ), an unphysical bound state with the S-matrix pole lying on the unphysical sheet. A characteristic cusplike structure around  $x \sim 0.15$  is caused when the virtual state acquires a finite width (also see Fig. 4). In contrast to the previous scenario with a complex meson-neutron scattering length, the  $i = 1$  channel pole in this model

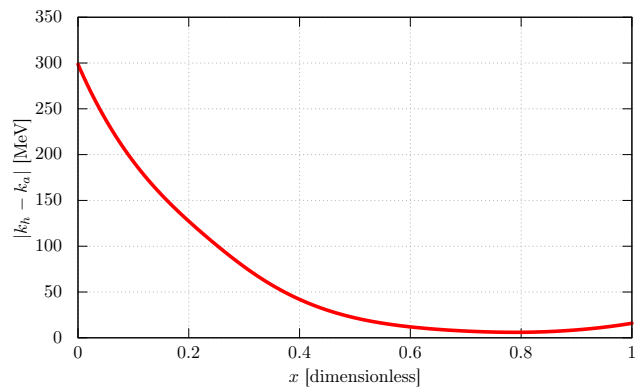


FIG. 5. Deviation of the eigenmomentum from the universal prediction  $|k_h - k_a|$  as a function of the extrapolation parameter  $x$  in the coupled-channel contact interaction model.

remains below the scattering threshold for any value of  $x$ , and in particular, the  $x = 0$  strangeness limit.

Thus, our simplistic model approach demonstrates that universality is a powerful tool to investigate the meson-neutron two-body system. In the next section, we consider the universal features in the three-body system consisting of two neutrons and one flavored meson, under the assumption that the two-body physics is essentially determined only by the scattering lengths that may be *finely tuned*. A low-energy EFT can provide a simple, but yet powerful systematic tool, for a quantitative analysis of such three-body systems in proximity to the scattering threshold. Incorporated with a renormalization group analysis of short-distance contact interactions (effective couplings), an EFT framework allows a natural mechanism of fine-tuning two-body parameters in order to probe the unitary (resonant), as well as the *scaling limits* in a low-energy three-body systems. In this way, complex three-body universal phenomena, such as the *Efimov effect* and the associated *discrete scaling symmetry*, are easily investigated within an EFT framework. Recently, a plethora of EFT based analyses have been used to predict the formation of bound states in a variety of three-body cluster states [37, 52–56].

### III. THREE-BODY SYSTEM OF TWO NEUTRONS AND ONE MESON

#### A. Effective field theory

We study the universality of a three-body system with  $J = 0$ ,  $I = 3/2$ , and  $I_3 = -3/2$ , consisting of two neutrons and one flavored meson. The magnitude of the two-body meson-neutron  $s$ -wave scattering length is tuned to a very large value while the  $s$ -wave neutron-neutron scattering length is kept fixed at the physical value. The scattering lengths in physical two-body systems like the  $K^-n$  or  $D^0n$  are generally untunable and fixed by nature.

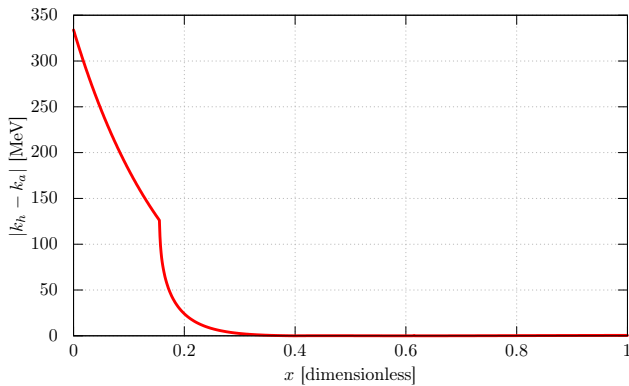


FIG. 6. Deviation of the eigenmomentum from the universal prediction  $|k_h - k_a|$  in the zero coupling limit as a function of the extrapolation parameter  $x$ .

The technique of extrapolating to the unphysical quark mass region, described in the previous section, provides us a viable mechanism to vary the scattering lengths and probe the universal physics. Primarily for the sake of a qualitative exploratory study, we shall henceforth neglect the sub-threshold decay channels  $i=2-4$ , which means that the meson-neutron scattering lengths can be taken to be real. In other words, our three-body analysis is consistent with the ZCL model assumption, though for the purpose of our following numerical study in the three-body sector, we shall consider the real parts of the results from the SIDDHARTA data analysis [i.e., from (1)] for kaon-neutron scattering length  $a_{0,K^-n}$ , and from the full contact interaction model [i.e., from (12)] for the  $D$ -meson-neutron scattering length  $a_{0,D^0n}$ , respectively,

$$\begin{aligned} a_{d(nK)} &= \text{Re} [a_{0,K^-n}] = -0.57 \text{ fm}, \\ a_{d(nD)} &= \text{Re} [a_{0,D^0n}] = 0.764 \text{ fm}. \end{aligned} \quad (22)$$

Our motivation of this part of the study is to determine under what circumstance do we expect to find the three-body system to become bound solely by virtue of the Efimov “attraction”. It is notable that complications arising due to additional Coulomb interactions is absent in this case which is essential for extracting universal information on bound systems. There is currently no consensus, both experimentally as well as theoretically, as to whether the system in the physical limits,  $x=0$  (i.e.,  $K^-nn$ ) and  $x=1$  ( $D^0nn$ ), respectively, are bound. Through universality based arguments in an EFT framework, we hope to gain insights alternative to rigorous realistic calculations, which is beyond the scope of the present work.

Here we shall employ a cluster effective field theory with a flavored meson field,  $K^-$  ( $D^0$ ), and a neutron field  $\psi_n$ , as the elementary degrees of freedom of the theory. We typically focus on low-energy threshold states far below the pion mass, i.e., the theory is *pionless*, with explicit pion degrees of freedom and their interaction effectively integrated out. The so-called *Kaplan-Savage-*

*Wise* (KSW) power counting rules [57, 58] incorporated with the *power divergence subtraction* scheme is most suitable for our purpose to renormalize the strongly interacting two-body sector and ensure unitarity for the finely-tuned system. In this section, we display the effective Lagrangian of the three-body system, where we denote the generic flavored meson field as  $K$  for brevity, but what it basically stands for is the flavor extrapolated meson field  $K(x)$ , implicitly dependent on the parameter  $0 \leq x \leq 1$ , discussed in the previous section. Note here that the actual meson charge is irrelevant in the context of the present analysis without Coulomb interaction, so that the change in the charge from the antikaon  $K^-$  (for  $x=0$ ) to the  $D^0$  meson (for  $x=1$ ) should not raise any concern.

For definiteness, we spell out the non-relativistic effective Lagrangian for the  $Knn$  system, consistent with the usual low-energy symmetries, like the parity invariance, charge conjugation, time-reversal invariance, and small velocity Lorentz invariance;

$$\mathcal{L} = \mathcal{L}_K + \mathcal{L}_n + \mathcal{L}_{d(nK)} + \mathcal{L}_{s(nn)} + \mathcal{L}_{3\text{-body}}. \quad (23)$$

The individual terms in the Lagrangian are elaborated in what follows. With the fundamental degrees of freedom as the neutron  $n$  and the flavor extrapolated meson  $K(x)$ , the single-particle Lagrangian at the leading order in the EFT is given by

$$\mathcal{L}_K = \phi_K^\dagger \left[ iv \cdot \partial + \frac{(v \cdot \partial)^2 - \partial^2}{2m_K} \right] \phi_K + \dots, \quad (24)$$

$$\mathcal{L}_n = \psi_n^\dagger \left[ iv \cdot \partial + \frac{(v \cdot \partial)^2 - \partial^2}{2M_n} \right] \psi_n + \dots, \quad (25)$$

with the 4-vector velocity  $v^\mu = (1, \mathbf{0})$ . The ellipsis stands for the higher order terms. The neutron field  $\psi_n$  is a two-component spinor representing a spin-doublet, while the flavored meson field  $K$  representing a spin-singlet. When the  $nn$  and  $nK$  scattering lengths are much larger than the typical length scales of short-range interactions, the two-body interactions can be expressed by means of contact terms:

$$\begin{aligned} \mathcal{L}_{2\text{-body}} &= -g_{nn} \left( \psi_n^T P_{(nn)}^{(1S_0)} \psi_n \right)^\dagger \left( \psi_n^T P_{(nn)}^{(1S_0)} \psi_n \right) \\ &\quad - g_{nK} \phi_K^\dagger \psi_n^\dagger \psi_n \phi_K + \dots, \end{aligned} \quad (26)$$

where the spin-singlet projection operator is defined as

$$P_{(nn)}^{(1S_0)} = -\frac{i}{2} \sigma_2. \quad (27)$$

It is, however, convenient for the description of three-body system to introduce the auxiliary *diatom* fields [31]: the spin-singlet *nn-dibaryon* field  $s_{(nn)}$ , and the spin-doublet *nK-dihadron* field  $d_{(nK)}$ . Moreover, it is often argued that in finely-tuned two-body sub-systems with threshold bound states, convergence of low-energy expansions can be significantly improved with such diatom

field trick [59, 60]. Thus, the  $s$ -wave two-body interactions Eq. (26) can be equivalently described by the Lagrangian

$$\mathcal{L}_{d(nK)} = \frac{1}{g_{nK}} d_{(nK)}^\dagger d_{(nK)} - \left[ d_{(nK)}^\dagger \psi_n \phi_K + \text{h.c.} \right] + \dots, \quad (28)$$

$$\mathcal{L}_{s(nn)} = \frac{1}{g_{nn}} s_{(nn)}^\dagger s_{(nn)} - \left[ s_{(nn)}^\dagger \left( \psi_n^T P_{(nn)}^{(1S_0)} \psi_n \right) + \text{h.c.} \right] + \dots. \quad (29)$$

Performing the renormalization in the two-body sector, we obtain the renormalized dihadron propagators for a generic center-of-mass momenta  $q = (q_0, \mathbf{q})$

$$S_d(q_0, \mathbf{q}) = \frac{2\pi}{\mu_{(nK)}} \frac{1}{\frac{1}{a_{d(nK)}} - \sqrt{-2\mu_{(nK)} \left( q_0 - \frac{q^2}{2(M_n + m_K)} \right) - i0^+}}, \quad (30)$$

$$S_s(q_0, \mathbf{q}) = \frac{4\pi}{M_n} \frac{1}{\frac{1}{a_{s(nn)}} - \sqrt{-M_n \left( q_0 - \frac{q^2}{4M_n} \right) - i0^+}}, \quad (31)$$

with the flavor extrapolated meson-neutron reduced mass  $\mu_{(nK)}(x) = M_n m_K(x) / (M_n + m_K(x))$ , and the  $s$ -wave scattering lengths  $a_{d(nK)}(x)$  and  $a_{s(nn)}$ , respectively, given as

$$\frac{1}{a_{d(nK)}} = \frac{2\pi}{\mu_{(nK)} g_{nK}}, \quad (32)$$

$$\frac{1}{a_{s(nn)}} = \frac{4\pi}{M_n g_{nn}}, \quad (33)$$

when the power divergence subtraction scheme is adopted. Note that the dihadron propagator is related to the  $s$ -wave two-body scattering amplitude with center-of-mass energy  $E_{\text{c.m.}}$  as  $f(E_{\text{c.m.}}) = -(2\pi/\mu_{(nK)}) S_d(E_{\text{c.m.}}, \mathbf{0})$ .

It is known that if the three-body system exhibits the Efimov effect, certain two-body interactions within the kernel of the three-body integral equations become ill-behaved in the asymptotic limit with the generic loop momenta  $q \rightarrow \infty$ . In this case the system of integral equations have no unique solutions. This problem is often ameliorated by introducing a sharp cut-off  $\Lambda$  in the integral equations. To renormalize possible non-analytic UV enhancement from the cut-off dependence, following the prescription mandated in Ref. [61], one must additionally include at the leading order a non-derivatively coupled three-body contact interaction. Such a three-body term in the Lagrangian, though formally power-counting sub-leading in a *naive dimensional* estimate, must be promoted to the leading order due to the above explained asymptotic enhancements. In our case, the three-body

Lagrangian is given as

$$\begin{aligned} \mathcal{L}_{\text{3-body}} &= \mathcal{L}_{nd(nK)}^{(1S_0)} + \dots, \\ \mathcal{L}_{nd(nK)}^{(1S_0)} &= -\frac{m_K g_s(\mu)}{\mu^2} \left( d_{(nK)}^T P_{(nd)}^{(1S_0)} \psi_n \right)^\dagger \\ &\quad \times \left( d_{(nK)}^T P_{(nd)}^{(1S_0)} \psi_n \right) + \dots, \end{aligned} \quad (34)$$

with the spin-singlet projection operator

$$P_{(nd)}^{(1S_0)} = -\frac{i}{\sqrt{2}} \sigma_2, \quad (35)$$

and  $g_s(\mu)$  is an *a priori* unknown three-body coupling that is required to be renormalized at a given momentum scale  $\mu$ . Note that here we have especially chosen to promote to the leading order, only the three-body interaction for the spin-singlet elastic channel, whereas the above ellipses correspond to other allowed three-body interaction terms in the EFT Lagrangian generally treated as sub-leading.

## B. Three-body integral equation

We now consider the integral equations for the three-body  $Knn$  system in the total spin-singlet channel. Such a system of equations can be constructed either by combining the dibaryon field  $s_{(nn)}$  and the flavor meson field  $K$ , or by combining the dihadron field  $d_{(nK)}$  and the neutron field  $n$ . The system of equations consists of two kinds of Faddeev-like partitions: a direct (elastic) hadron exchange channel  $nd_{(nK)} \rightarrow nd_{(nK)}$  (denoted as  $t_a$ ), and a hadron rearrangement (inelastic) channel  $nd_{(nK)} \rightarrow s_{(nn)}K$  (denoted as  $t_b$ ). For concreteness, the coupled-channel three-body equation for the *half-off-shell* amplitudes  $t_a$  and  $t_b$  is diagrammatically displayed in Fig. 7 [37].

It is straightforward to obtain this equation following the Feynman rules from the Lagrangian presented in the previous subsection. After the  $s$ -wave projection, we obtain

$$\begin{aligned} &t_a(p', p; E) \\ &= \frac{m_K}{2p'p} \ln \left[ \frac{p'^2 + p^2 + ap'p - 2\mu_{(nK)}E}{p'^2 + p^2 - ap'p - 2\mu_{(nK)}E} \right] \\ &\quad - \frac{m_K}{2\mu_{(nK)}\pi} \int_0^\Lambda dl \frac{l}{p'} \ln \left[ \frac{p'^2 + l^2 + ap'l - 2\mu_{(nK)}E}{p'^2 + l^2 - ap'l - 2\mu_{(nK)}E} \right] \\ &\quad \times \frac{t_a(l, p; E)}{\frac{1}{a_{d(nK)}} - \sqrt{-2\mu_{(nK)}E + \frac{\mu_{(nK)}}{M_n} l^2 - i0^+}} \\ &\quad - \frac{\sqrt{2}}{\pi} \int_0^\Lambda dl \frac{l}{p'} \ln \left[ \frac{p'^2 + bl^2 + p'l - M_n E}{p'^2 + bl^2 - p'l - M_n E} \right] \\ &\quad \times \frac{t_b(l, p; E)}{\frac{1}{a_{s(nn)}} - \sqrt{-M_n E + \frac{M_n}{2\mu_{K(nn)}} l^2 - i0^+}}, \end{aligned} \quad (36)$$

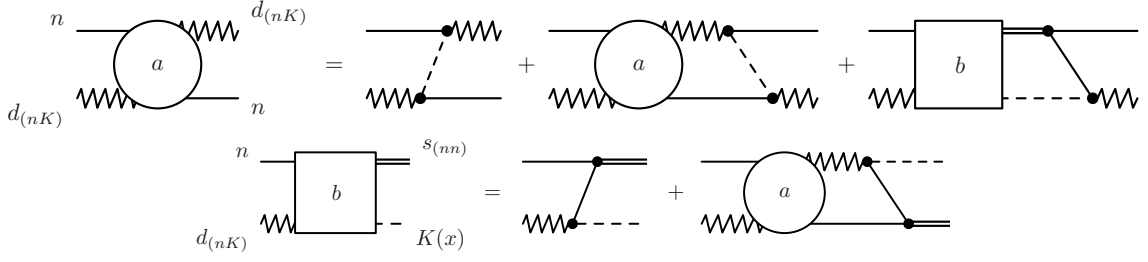


FIG. 7. Feynman diagrams for the three-body coupled integral equations. Solid and dashed lines represent the bare propagators of  $n$  and  $K(x)$ , respectively, and double and zigzag lines stand for the dressed propagators of  $s_{(nn)}$  and  $d_{(nK)}$ , respectively.

and

$$\begin{aligned}
& t_b(p', p; E) \\
&= \frac{M_n}{\sqrt{2}p'p} \ln \left[ \frac{bp'^2 + p^2 + p'p - M_n E}{bp'^2 + p^2 - p'p - M_n E} \right] \\
&\quad - \frac{M_n}{\sqrt{2}\pi\mu_{(nK)}} \int_0^\Lambda dl \frac{l}{p'} \ln \left[ \frac{bp'^2 + l^2 + p'l - M_n E}{bp'^2 + l^2 - p'l - M_n E} \right] \\
&\quad \times \frac{t_a(l, p; E)}{\frac{1}{a_{d(nK)}} - \sqrt{-2\mu_{(nK)}E + \frac{\mu_{(nK)}}{\mu_{n(nK)}}l^2 - i0^+}}, \tag{37}
\end{aligned}$$

where  $E$  is the total center-of-mass kinetic energy of the three-body system,  $p$  and  $p'$  are the initial and final state momenta,  $\mu_{n(nK)} = M_n(M_n + m_K(x))/(2M_n + m_K(x))$ , and we have defined the two mass dependent parameters

$$a(x) = \frac{2\mu_{(nK)}(x)}{m_K(x)}, \quad b(x) = \frac{M_n}{2\mu_{(nK)}(x)}, \tag{38}$$

where we re-emphasized their dependence on the value of extrapolation parameter at a general unphysical point  $x \neq 0, 1$ . Moreover, note that the amplitude  $t_b$  is dependent only on  $t_a$  and not itself, which means that the coupled equations could be reduced to a single equation for  $t_a$  after substituting the Eq. (37) for  $t_b$  in Eq. (36). The coupled integral equations are numerically solved to obtain the non-perturbative solutions to the three-body problem. It is important to note that these integral equations must be regularized, e.g., by introducing a sharp momentum cut-off  $\Lambda$  to remove any ambiguity in the phase of asymptotic solution with the cut-off taken to infinity [61, 62], wherever the system exhibits the Efimov effect. An asymptotic analysis in the following subsection shows that this is indeed the case in the present problem. Thus, the resulting prediction though unique exhibits a log-periodic dependence  $\propto \ln(\Lambda)$ . This dependence is further renormalized at the cut-off scale  $\mu = \Lambda$  by introducing the leading order three-body contact interaction term in the Lagrangian displayed in Eq. (34) with a cut-off dependent running coupling  $g_s(\mu = \Lambda)$ .

### C. Asymptotic expression

In order to determine whether the three-body system exhibits the Efimov effect, it is instructive to examine the asymptotic expression for the integral equation for  $t_a$  [31] with the cut-off removed, i.e.,  $\Lambda \rightarrow \infty$ . For this purpose, if we consider a three-body bound state energy at  $E = -B_d < 0$ , then the three-body amplitude should be dominated by the S-matrix pole term:

$$t_a(p', p; E) \simeq \frac{z(p')z(p)}{(E + B_d)} + \dots (\text{regular terms}), \tag{39}$$

where the residue factors into the *pseudo-wavefunctions* in the momentum space  $z(p)$  and  $z(p')$ , respectively. Because the bound state solution satisfies the homogeneous integral equations, the problem can be reduced to an integral equation for  $z(p')$ . This is because in the asymptotic regime, we consider the scale of the momentum  $p'$  to be very large in comparison with the inverse two-body scattering lengths and the eigenenergies of the bound state, i.e.,  $p', l \gg 1/a_{d(nK)}, 1/a_{s(nn)}, \sqrt{2\mu_{(nK)}B_d}, \sqrt{M_n B_d}$ . The integral equations for  $t_a$  and  $t_b$  in this regime can then be combined into a single equation that reads

$$\begin{aligned}
z(p') &= C_1 \int_0^\infty dl \frac{z(l)}{p'} \ln \left[ \frac{p'^2 + l^2 + ap'l}{p'^2 + l^2 - ap'l} \right] \\
&\quad + C_2 \int_0^\infty dl \frac{1}{p'} \ln \left[ \frac{p'^2 + bl^2 + p'l}{p'^2 + bl^2 - p'l} \right] \\
&\quad \times \int_0^\infty dk \frac{z(k)}{l} \ln \left[ \frac{k^2 + bl^2 + kl}{k^2 + bl^2 - kl} \right]. \tag{40}
\end{aligned}$$

with

$$C_1 = \frac{(M_n + m_K)^2}{2\pi M_n \sqrt{m_K(2M_n + m_K)}}, \tag{41}$$

$$C_2 = \frac{2(M_n + m_K)^2}{\pi^2 m_K(2M_n + m_K)}. \tag{42}$$

It is notable that the solution to the above equation has a  $z(p') \rightarrow z(p_*^2/p')$  symmetry for arbitrary real parameter  $p_*$  containing the information on the asymptotic phase [61]. Because of this inversion symmetry, the solutions always come in pairs.

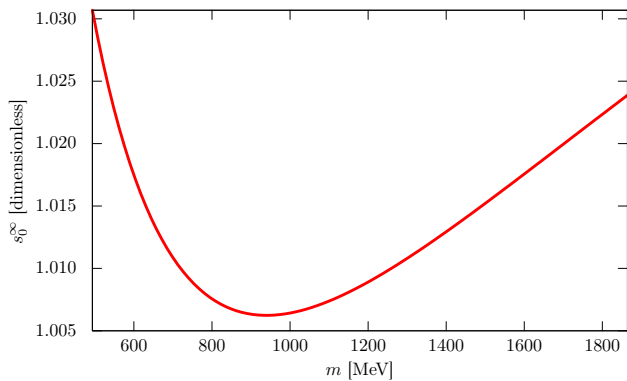


FIG. 8. Flavored meson mass dependence on the asymptotic parameter  $s_0^\infty$  for  $m_{K^-} < m < m_{D^0}$ .

The absence of a scale dependence in the above equation, the solution is expected to follow a power law:  $z(p') \propto p'^{s-1}$ . The integral equation now reduces to a simple algebraic (transcendental) equation for the exponent  $s$ , which reads

$$1 = C_1 I_0(s) + C_2 I_1(s) I_2(s) \quad (43)$$

where

$$I_0(s; a) = \frac{2\pi}{s} \frac{\sin[s \arcsin(a/2)]}{\cos(\pi s/2)}, \quad (44)$$

$$I_1(s; b) = \frac{2\pi}{s} \frac{1}{b^{s/2}} \frac{\sin[s \operatorname{arccot}(\sqrt{4b-1})]}{\cos(\pi s/2)}, \quad (45)$$

$$I_2(s; b) = b^s I_1(s; b). \quad (46)$$

It is known that the original integral equation is ill-defined when this algebraic equation has a pair of imaginary solutions  $s = \pm i s_0^\infty$ , with  $s_0^\infty$  being a transcendental number. By using the meson masses in the physical limits, i.e., for the antikaon  $K^-(x=0)$  and the charmed meson  $D^0(x=1)$ , as given in Table I, we indeed obtain such imaginary solutions with

$$s_0^\infty = \begin{cases} 1.03069 & \text{for } K^- nn, \\ 1.02387 & \text{for } D^0 nn. \end{cases} \quad (47)$$

In fact, imaginary solutions to Eq. (43) are continuously obtained by extrapolating the flavored meson mass  $m \equiv m_K(x)$  in between the physical limits  $m_{K^-}(x=0)$  and  $m_{D^0}(x=1)$ , as depicted in Fig. 8. We thereby conclude that the Efimov effect must occur in the meson-neutron-neutron three-body system at the intermediate unphysical point  $x \sim 0.615$ , when the two-body sub-system is tuned to the unitary limit with  $a_{d(nK)}, a_{s(nn)} \rightarrow \infty$ .

Although not directly relevant in the context of the non-asymptotic analysis that we present in the following subsection, it is somewhat instructive to consider another interesting limit of the three-body problem with only  $a_{d(nK)}(x)$  tuned infinitely large as  $x \rightarrow 0.615$ . In comparison, the physical value of the spin-singlet  $s$ -wave  $nn$

scattering length  $a_{s(nn)} = -18.63$  fm [63] can be regarded as a small quantity, even though in reality  $|a_{s(nn)}|$  itself is much larger than the length scale in the strong interaction. Thus, if we can consider the limit  $a_{d(nK)}(x) \rightarrow \infty$  with fixed  $a_{s(nn)} \sim 0$ , the dineutron propagator is completely suppressed in comparison to the  $d_{(nK)}$  dihadron propagator, and the corresponding asymptotic equation for the exponent  $s$  is simply reduced to

$$1 = C_1 I_0(s; a). \quad (48)$$

This transcendental equation still yields a pair of the imaginary solutions  $s = \pm i s_0'^\infty$  with

$$s_0'^\infty = 0.327675 \quad (49)$$

at  $x \sim 0.615$  with the extrapolated meson mass  $m_K(x) \sim 1336.61$  MeV. Thus, it is interesting to see that the Efimov effect in the three-body system also surviving in this special limit, although the Efimov “attraction” in this limit is likely to become considerably weak leading to a very sparse Efimov spectrum.

#### D. Including genuine three-body force

As an upshot to the previous asymptotic analysis, a three-body force contribution becomes clearly necessary in the EFT framework. Here we include a *genuine* three-body contact interaction proportional to the running couplings  $g_s(\Lambda)$ , where the renormalization scale is set to  $\mu = \Lambda$ , the sharp momentum cut-off introduced in the integral equations. As the three-body system exhibits the Efimov effect, an RG analysis of the coupling  $g_s(\Lambda)$  is likely to yield a limit cycle in the asymptotic regime. As per the basic EFT tenet, the presence of an asymptotic limit cycle gives us the freedom to choose any one of the channels to promote the corresponding three-body interaction terms to the leading order. In this analysis, we choose to modify the amplitude  $t_a$  for the elastic channel  $nd_{(nK)} \rightarrow nd_{(nK)}$ , which in turn modifies the two-body meson exchange interaction:

$$K_{(K)}(p', p; E) \rightarrow K_{(K)}(p', p; E) - \frac{g_s(\Lambda)}{\Lambda^2}, \quad (50)$$

where

$$K_{(K)}(p', p; E) = \frac{1}{2pp'} \ln \left[ \frac{p'^2 + p^2 + ap'p - 2\mu_{(nK)}E}{p'^2 + p^2 - ap'p - 2\mu_{(nK)}E} \right]. \quad (51)$$

With this modification, we hope to shed light whether the limit cycle RG of the coupling  $g_s$  is likely to survive in the low-energy non-asymptotic regime.

#### E. Numerical results

As already mentioned, the numerical evaluations of the integral equation require the meson-neutron and

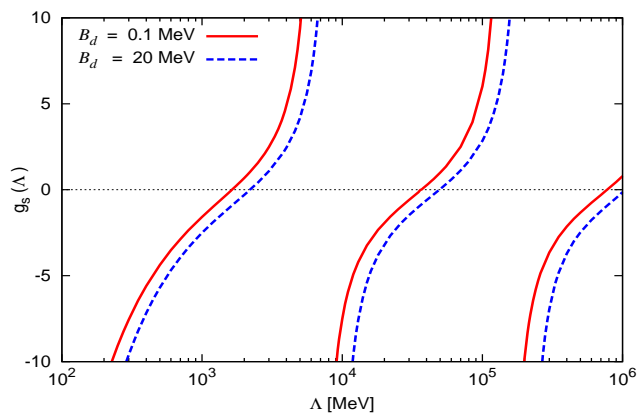


FIG. 9. Limit cycle RG for the three-body coupling  $g_s$  as a function of the sharp momentum cut-off  $\Lambda$  for the  $K^-nn$  trimer. The pertinent integral equations are solved with the two-body scattering lengths, as given in Eq. (22), as the input for fixed trimer eigenenergies of  $B_d = 0.1$  MeV and 20 MeV.

neutron-neutron  $s$ -wave scattering lengths as the principal inputs in our leading order EFT analysis employed in this work. Firstly, our numerical results are displayed with the spin-singlet  $s$ -wave  $nn$  scattering length taken as the physical value,  $a_{s(nn)} = -18.63$  fm [63]. Secondly, two different sets of meson-neutron scattering lengths are used. Unless explicitly stated otherwise, we use the real parts of the otherwise complex meson-neutron scattering lengths, as displayed in Eq. (22). However, when the three-body system is extrapolated to the unphysical region  $0 < x < 1$ , to investigate the universality around the unitary limit, it is more intuitive to use the ZCL model with the scattering lengths as obtained in Fig. 3. We solve the non-asymptotic form of the integral equations (36) and (37) for the amplitude  $t_a$  to obtain the three-body energy eigenvalue as a function of the sharp cut-off  $\Lambda$ .

We first include the three-body force containing the  $g_s(\Lambda)$  term, to investigate whether the limit cycle nature is manifested in the  $K^-nn$  system at non-asymptotic momenta/energies. Later we focus on the results without including the the three-body term to investigate the behavior of the binding energies of the  $K^-nn$  and  $D^0nn$  three-body systems (i.e., at  $x = 0$  and 1) generated exclusively from the two-body dynamics. In particular, the role of the cut-off ( $\Lambda$ ) dependence of the results is investigated which can crucially determine whether the three-body bound state formation is supported in the framework of the low-energy EFT. Further in the context of the ZCL model, a study of the first “critical” cut-off  $\Lambda_c^{(n=0)}$  (as defined later) is presented whose variation as a function of the extrapolation parameter  $x$  between the strangeness and charm sectors reveals vital information on the three-body universal characteristics. These in association with our earlier findings in the two-body sector is used to predict the likely-hood of realistic Efimov-like

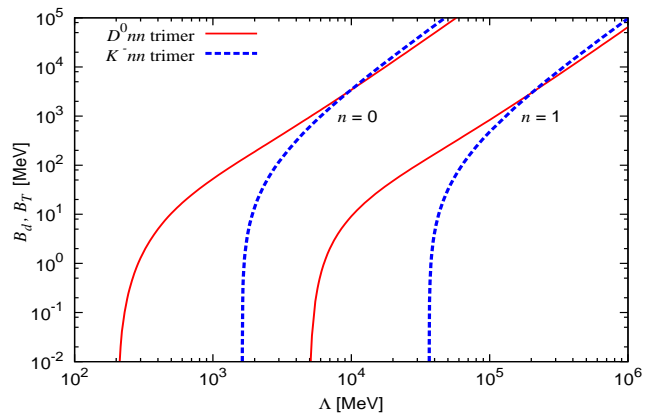


FIG. 10. Trimer binding energies for the ground ( $n = 0$ ) and first ( $n = 1$ ) excited Efimov-like level states as a function of the sharp momentum cut-off  $\Lambda$ , excluding the three-body force. The pertinent integral equations are solved with the two-body scattering lengths as given in Eq. (22) as the input. For the  $K^-nn$  system, the trimer binding energy  $B_d$  is measured with respect to the three-particle breakup threshold, while for the  $D^0nn$  system the binding energy  $B_T = B_d - E_D$  is measured with respect to the particle-dimer breakup threshold energy  $E_D = 53.4$  MeV.

bound states.<sup>3</sup>

We then present our result for the limit cycle RG, e.g., in the  $K^-nn$  system by including the genuine three-body contact interaction containing the scale dependent coupling  $g_s(\Lambda)$ . For a proper estimation of this coupling a knowledge of a three-body observable, such as the  $s$ -wave particle-dimer scattering length or the trimer binding energy is required, neither of which is currently available. However, even in the absence of such three-body datum, we may still study the scale evolution or the renormalization group behavior of this coupling by fixing any presumably small value of the trimer binding energy, say  $B_d \sim 0.1$  MeV, and varying the cut-off scale  $\Lambda$ . Various qualitative features concerning three-body universality can be deduced thereof.

Fig. 9, demonstrates the typical cyclic periodicity of a limit cycle for the coupling  $g_s(\Lambda)$  for the  $K^-nn$  system. The periodic divergence of the coupling is associated with the formation of three-body bound states. The qualitative feature of the plot remains unchanged whether the binding energy is chosen close to the threshold as above, or somewhat away from threshold with a larger binding energy, say,  $B_d \sim 20$  MeV; there is only a downward shift of each curve with increasing  $B_d$  because the interaction becomes more attractive with larger binding energies.

For the running coupling  $g_s(\Lambda)$ , the characteristic pe-

<sup>3</sup> A brief description of our numerically methodology of solving the integral equations is presented in Appendix A.

riodicity, with  $\Lambda = \Lambda^{(N)} \forall N \in \mathbb{N}$ , can be expressed as

$$g_s(\Lambda^{(1)}) = g_s(\Lambda^{(N+1)}) \quad \text{with } \Lambda^{(N+1)} = \Lambda^{(1)} \exp\left(\frac{N\pi}{s_0}\right), \quad (52)$$

where  $s_0$  is a real three-body parameter reminiscent of the corresponding asymptotic limit cycle value of  $s_0^\infty = 1.03069$  we found earlier, and is a measure of an approximate discrete scale invariance of the three-body system. In particular, the running coupling vanishes quasi-periodically at a discrete set of cut-off values expressed as  $\Lambda_0^{(N+1)} = \Lambda_0^{(1)} \exp\left(\frac{N\pi}{s_0}\right)$ . It is notable that  $s_0^\infty$  is an universal number, depending only on the ratios of the respective masses of the three bound particles. While the non-universal number  $s_0$  deviates from  $s_0^\infty$  primarily due to cut-off dependent effects, implying an implicit dependence on  $N$  itself, i.e.,  $s_0 \equiv s_0^{(N)}$ . Additional non-asymptotic parametric dependence on the binding energy  $B_d$ , three-body coupling  $g_s$  and the two-body scattering lengths, can further influence the numerical value of  $s_0^{(N)}$ . In other words,  $s_0^{(N)}$  being an outcome of a numerical RG is purely numerical by nature and thereby difficult to ascribe a unique definition. However, a reasonably good estimates could be obtained by taking the successive discrete cut-offs, say,  $\Lambda_0^{(N)}$  and  $\Lambda_0^{(N)}$  for the vanishing coupling  $g_s(\Lambda_0^{(N)}) = 0$ , and using the closed-form definition:

$$s_0^{(N)} = \frac{\pi}{\ln\left(\frac{\Lambda_0^{(N+1)}}{\Lambda_0^{(N)}}\right)}. \quad (53)$$

A crucial observation in this definition is that the sequence of non-asymptotic numbers  $s_0^{(N)}$  obtained above gradually converges to the asymptotic value  $s_0^\infty$  beyond a suitably large  $N > 0$ . Mathematically, stated otherwise: for  $\epsilon > 0$ ,  $\exists N_0 \in \mathbb{N}$ , such that

$$\left|s_0^{(N)} - s_0^\infty\right| < \epsilon, \quad \forall N > N_0. \quad (54)$$

An alternative method of extraction of the  $s_0$  parameter is presented in Appendix B.

In the following numerical study, we shall exclude the three-body force since there is no three-body input available to fix the coupling  $g_s$ . In Fig. 10, the result for the trimer energy of the physical systems  $K^-nn$  ( $x = 0$ ) and  $D^0nn$  ( $x = 1$ ) are summarized. In the figure, the ground ( $n = 0$ ) and the first excited ( $n = 1$ ) binding energies  $-E = B_d > 0$  of the  $K^-nn$  trimer Borromean [32] system, with  $a_{d(nK)}, a_{s(nn)} < 0$ , measured with respect to the three-particle breakup threshold, are plotted as a function of  $\Lambda$ . The same figure also displays the corresponding eigenenergies  $B_T = B_d - E_D$  of the  $D^0nn$  trimer state, measured with respect to the particle-dimer breakup ( $n + D^0n$ ) threshold, with the two-body  $D^0n$  binding energy,

$$E_D = \frac{1}{2\mu_{(nD)}a_{d(nD)}^2}, \quad (55)$$

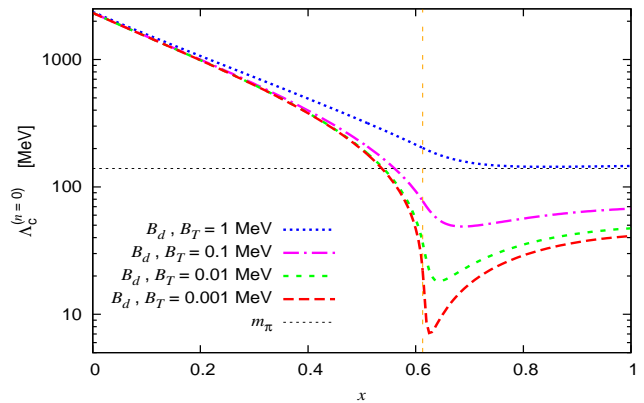


FIG. 11. Extrapolation of the critical cut-off  $\Lambda_c^{(0)}$ , associated with the  $n = 0$  Efimov-like ground state for fixed trimer binding energies  $B_d(B_T)$  of the meson-neutron-neutron bound state, measured along the three-particle (particle-dimer) break-up threshold. The double dashed vertical line at  $x \sim 0.615$  denotes the unitary limit. The plot corresponds to the case of the zero coupling approximation (ZCL model) with input scattering lengths as in Eq. (19).

which is obtained as  $E = -E_D \simeq -53.4$  MeV, using the value of  $a_{d(nD)}$  in Eq. (22). This is to be contrasted with the corresponding value of the  $D^0n$  virtual state pole position on the complex energy plane  $E_h = -3.9 - i36.0$  MeV, obtained in the coupled-channel contact interaction model (see Fig. 2).

Both the above plots clearly indicate the increasing magnitude of the binding energies as the cut-off scale  $\Lambda$  is increased. The sensitivity of the low-energy result to the cut-off variation is a typical indication akin to the asymptotic Efimov states, which evidently survive in the non-asymptotic regime in the context of our simplistic picture with finite scattering lengths, albeit the neglect of the imaginary part of the scattering lengths. Equivalently, this amounts to decreasing the range of the three-body interactions eventually leading to the well-known “fall to the center” pathology, so-called the *Thomas collapse* [64], an artifact of the three-body system in the zero-range scaling limit. In the figure, the first branch refers to the Efimov-like ground state for the  $K^-nn$  ( $D^0nn$ ) system, which appears as a shallow threshold state at the so-called “critical” cut-off value of  $\Lambda_c^{(n=0)} \simeq 1.6$  GeV ( $\simeq 204$  MeV). This state becomes increasingly deeply bound with increasing cut-off, while the second branch, i.e., the first excited state appears at the critical value  $\Lambda_c^{(n=1)} \simeq 36.5$  GeV ( $\simeq 5$  GeV), which in its turn gets progressively deeper. Continuing in this manner an infinite tower of excited states emerge from the the zero energy threshold as  $\Lambda \rightarrow \infty$ .

Let us now revisit the ZCL model and study the extrapolation of the  $K^-nn$  system in the  $x = 0$  limit to the  $D^0nn$  system in the  $x = 1$  limit, where the scattering lengths of the  $K^-n$  and  $D^0n$  systems are modified as shown in Eq. (19). As already seen in Sec. IIC, a

continuous extrapolation of the meson-neutron system from  $K^-n$  to  $D^0n$  (see Fig. 3) using the ZCL model yielded an unitary limit of the meson-neutron interaction in the proximity of  $x \sim 0.615$ . Here we investigate the behavior of the “critical point”  $\Lambda_c^{(0)}$ , corresponding to  $n = 0$  ground state of the meson-neutron-neutron three-body system, as a function of the extrapolation  $x$  between its two physical limits for fixed trimer energy  $B_d$  or  $B_T$ .<sup>4</sup> In other words, we perform an extrapolation in the interval  $x = [0, 0.615)$ , i.e., along the three-particle break-up threshold with a fixed value of  $B_d$ , and continue further in the interval  $x = (0.615, 1]$ , i.e., along the particle-dimer break-up threshold with a fixed value of  $B_T = B_d - E_D(x)$  where  $E_D$  in the latter interval varies as a function of  $x$ . Level energies chosen too close to the thresholds can lead to numerical instabilities in the vicinity of the unitary limit. We have, therefore, preferred non-zero binding energies  $B_d, B_T \geq 0.001$  MeV suitable our purpose of demonstration.

Fig. 11 displays the results in the context of the ZCL model where the meson mass and the  $s$ -wave meson-neutron (inverse) scattering length are simultaneously extrapolated from  $x = 0$  to  $x = 1$ . The fact that there is a large change (about 3 orders of magnitude) in the critical cut-off along  $x = [0, 0.615)$  compared to a rather nominal change along  $x = (0.615, 1]$ , suggests that the  $D^0nn$  system is much more likely to be found in the domain of three-body universality and yield a bound state than the  $K^-nn$  system. The horizontal dotted line in the above figure indicates the one-pion threshold, the upper cut-off of the pionless EFT employed in this analysis. A direct comparison with the behavior of the critical cut-off indicates that a bound  $D^0nn$  ground state is clearly supported in the realm of the low-energy EFT framework, lying well below the hard scale  $\Lambda_{\not{p}} \sim m_\pi$ , while the same for the  $K^-nn$  system lies far above the applicability of the EFT, and thus, can be considered unbound.

#### IV. DISCUSSION AND SUMMARY

In this work, we have explored the two and three-body universal physics associated with a three-particle cluster state of two neutrons and a flavored meson i.e., an antikaon  $K^-$  or a  $D^0$  meson. The technique of extrapolation to unphysical quark masses between the strange and the charm flavors, provides a natural mechanism to tune the meson-neutron interaction close to resonant conditions where the corresponding two-body scattering length can reach very large values. However, much of the universal physics under resonant condition gets obscured by

coupled channel effects of sub-threshold decay channels. It is, thus, intuitive to consider the scenario where the channel coupling are switched off. This is the so-called zero coupling limit of the Weinberg-Tomozawa contact interaction model which is used at first to investigate the extrapolation in meson-neutron  $s$ -wave interactions. To explore the universal region the extrapolation parameter  $x$  is continuously varied in the range  $0 \leq x \leq 1$ , between the two physical limits of  $K^-n$  ( $x = 0$ ) and  $D^0n$  ( $x = 1$ ). This led to the identification of the entire region  $x \gtrsim 0.3$  as the two-body universal window, and in particular, obtain the unitary limit of the meson-neutron interaction at  $x \sim 0.615$ , as elucidated in Fig. 6. One can then conclude that physical  $D^0n$  system lying in the neighborhood of the universal region is more likely to follow the predictions of universality than its strangeness counterpart  $K^-n$ , located far outside this region.

Next, to investigate the three-body universality we employ a low-energy cluster EFT. In a simplified approach, we again neglect the influence of sub-threshold decay channels which amounts to considering the  $s$ -wave meson-neutron scattering lengths to be real. A leading order EFT analysis allows us to investigate the meson-neutron-neutron system in the scaling limit (zero-range approximation) where the universal physics is determined only by the two  $s$ -wave scattering lengths  $a_{d(nK)}$  and  $a_{s(nn)}$ . In this work,  $a_{s(nn)}$  is kept fixed to the physical value, while  $a_{d(nK)} \equiv a_{d(nK)}(x)$  is varied as a function of  $x$  to probe the meson-neutron unitarity and study its consequences in the Efimov-like bound state formation. The introduction of a sharp momentum cut-off  $\Lambda$  in the integral equations leads to a scale violation resulting in a discrete scaling invariance in the asymptotic region.

We first confirm an approximate limit cycle RG (with quasi-log-periodicity) of the three-body running coupling  $g_s(\Lambda)$  for the  $K^-nn$  system, as evident in Fig. 9. A very similar feature is also exhibited by the  $D^0nn$  system which we do not display in this article. Moreover, Fig. 8 suggests that the asymptotic limit cycle between the  $K^-nn$  and  $D^0nn$  systems continuously exists for all intermediate  $x$  in the sense that the respective asymptotic parameters  $s_0^\infty = 1.03069$  and  $s_0^\infty = 1.02387$  are smoothly connected. This leads to the conclusion that the Efimov effect is indeed manifested in the three-body system at the unphysical point  $x \sim 0.615$ , when the meson-neutron sub-system reaches the unitary limit.

The binding energy  $B_d$  for the  $K^-nn$  system and  $B_T$  for the  $D^0nn$  system are calculated as a function of the cut-off  $\Lambda$  using the real parts of the two-body  $s$ -wave scattering lengths in each channel, as displayed in Fig. 10. For the sake of simplicity we exclude the dependence on the three-body force with the unknown coupling  $g_s$ . We find that the binding energies increase with increasing  $\Lambda$ , and the various Efimov-like level states emerge in order from the zero energy threshold, starting from a deepest (ground) state that appears at a certain critical value  $\Lambda_c^{(0)}$ . Evidently, a larger value of the cut-off leads to additional inclusion of ultraviolet physics into the the-

<sup>4</sup> Because here we do not explicitly include the three-body force, the critical point  $\Lambda_c^{(n=0)}$  corresponds to the first zero of the three-body coupling, i.e.,  $g_s(\Lambda_0^{(N=1)}) = 0$  in Fig. 9, for a fixed binding energy  $B_d$  or  $B_T$ .

ory from high energy modes leading to greater attraction in the system and consequently result in larger three-body binding energies and emergence of new level states. With much smaller critical cut-offs for the level states of the  $D^0nn$  system than those of the  $K^-nn$  system it is straightforward to conclude that the  $D^0nn$  trimer states are manifested more easily.

Finally, in Fig. 11, the lowest critical cut-off  $\Lambda_c^{(0)}$ , associated with the emergence of the Efimov-like ground state near threshold, is calculated as a function of  $x$  using the extrapolated inverse meson-neutron scattering length  $1/a_0$  (shown in Fig. 3) in the ZCL model. Clearly as the values of  $B_d$  or  $B_T$  become smaller,  $\Lambda_c^{(0)}$  converges to the point, ( $x \simeq 0.615, \Lambda_c^{(0)} \simeq 0$ ), at which Efimov states are realized with vanishing scale in the two-body sector. As the parameter  $x$  goes toward the physical limits, i.e.,  $x = 0$  and  $x = 1$ ,  $\Lambda_c^{(0)}$  becomes larger, indicating that a larger strength of interaction is necessary to form bound states in the three-body system. However, one also sees that in the  $x = 1$  physical limit, the  $D^0nn$  system is much closer to the unitary limit at  $x \simeq 0.615$  than in the  $x = 0$  physical limit of the  $K^-nn$  system. Thus, a plausible  $D^0nn$  ground state trimer can especially be realized within the pionless EFT framework with  $\Lambda_c^{(0)}$  lying much below the pion mass. While for the  $K^-nn$  system, with  $\Lambda_c^{(0)} \gtrsim 2000$  MeV, no physically realizable mechanism in the context of a low-energy EFT can generate sufficient interaction strength to form bound states.

Having said that, it must also be borne in mind that the dynamics of the sub-threshold decay channels that are systematically neglected in the three-body analysis presented in this work, may play vital role to ultimately decide the fate and nature of the Efimov states. Given the large threshold energy difference ( $\sim 210$  MeV) and the coupling constants being suppressed by the  $\kappa$  factor in the  $D^0nn$  sector, the primary effect of the neglected channels would simply contribute to a finite decay width to the three-body bound states found in our analysis. Nevertheless, the dynamical effect of the decay channel should be checked in a more robust coupled channel framework. In regard to drawing definitive conclusions, the EFT framework should either be elaborated by including sub-leading order effects, such as the effective range corrections, or by employing rigorous few-body technique combined with the realistic two-body potentials. Thus, in conclusion, our simplistic analysis raises the intriguing possibility of Efimov mechanism playing vital role in neutron rich three-body systems with at least one flavored meson toward formation of exotic bound states. Hopefully, this opens up the opportunity to further investigate the exact character of  $K^-nn$  system, and to ascertain whether the ground state of the  $D^0nn$  system, if bound, does qualify for an Efimov state.

## Appendix A: Solution via numerical integration

We present here some details of the methodology used in this work to numerically solve the integral equations (36) and (37) in order to obtain the three-body energy eigenvalues  $-E = B_d > 0$ , as a function of the sharp momentum cut-off  $\Lambda$ . For this purpose, we are only required to solve the homogeneous version of the coupled integral equations written in the general linearized form

$$\begin{aligned} t_a &= A \otimes t_a + B \otimes t_b, \\ t_b &= C \otimes t_a + D \otimes t_b, \end{aligned} \quad (\text{A1})$$

or equivalently,

$$[x] = \mathbf{X} \otimes [x] \quad (\text{A2})$$

with  $[x]$ , the column eigenvector and  $\mathbf{X}$ , the transformation matrix, defined as

$$[x] = \begin{bmatrix} t_a \\ t_b \end{bmatrix}, \quad \mathbf{X} = \begin{bmatrix} A & B \\ C & D \end{bmatrix}. \quad (\text{A3})$$

In the present problem the elements of the  $2 \times 2$  transformation matrix  $\mathbf{X}(p', l)$  are given by

$$\begin{aligned} A(p', l) &= \frac{m_K}{\pi \mu_{(nK)}} \frac{l^2 K_{(K)}(p', l; E)}{\left[ -\frac{1}{a_{d(nK)}} + \sqrt{\frac{\mu_{(nK)}}{\mu_{n(nK)}} l^2 - 2\mu_{(nK)} E} \right]}, \\ B(p', l) &= \frac{2\sqrt{2}}{\pi} \frac{l^2 K_{(n1)}(p', l; E)}{\left[ -\frac{1}{a_{s(nn)}} + \sqrt{\frac{M_n}{2\mu_{K(nn)}} l^2 - M_n E} \right]}, \\ C(p', l) &= \frac{\sqrt{2} M_n}{\pi \mu_{(nK)}} \frac{l^2 K_{(n2)}(p', l; E)}{\left[ -\frac{1}{a_{d(nK)}} + \sqrt{\frac{\mu_{(nK)}}{\mu_{n(nK)}} l^2 - 2\mu_{(nK)} E} \right]}, \\ D(p', l) &= 0. \end{aligned} \quad (\text{A4})$$

where the  $s$ -wave projected one-meson exchange propagator is given by

$$K_{(K)}(p', l; E) = \frac{1}{2lp'} \ln \left( \frac{p'^2 + l^2 + ap'l - 2\mu_{(nK)} E}{p'^2 + l^2 - ap'l - 2\mu_{(nK)} E} \right), \quad (\text{A5})$$

while the one-neutron exchange interaction for the elastic and inelastic channels are parameterized by the two propagators:

$$\begin{aligned} K_{(n1)}(p', l; E) &= \frac{1}{2lp'} \ln \left( \frac{p'^2 + bl^2 + p'l - M_n E}{p'^2 + bl^2 - p'l - M_n E} \right), \\ K_{(n2)}(p', l; E) &= \frac{1}{2lp'} \ln \left( \frac{bp'^2 + l^2 + p'l - M_n E}{bp'^2 + l^2 - p'l - M_n E} \right). \end{aligned} \quad (\text{A6})$$

The integration are evaluated employing the method of Gaussian quadrature where the integral over the loop momentum variable  $l$  is replaced by a summation over  $N$

Gauss-Legendre weights  $w_j$ , and correspondingly choosing  $N \times N$  intermediate mesh points  $(p'_i, l_j)$  between the integration limits  $[0, \Lambda]$ , i.e.,

$$\otimes \equiv \int_0^\Lambda dl \rightarrow \sum_{j=0}^N w_j. \quad (\text{A7})$$

To achieve better numerical convergence with a relatively small number of quadrature points, say,  $N = 96$ , we find it convenient to reparameterize the integration variable in the following way: First we assume that the momenta  $l, \Lambda$  be re-scaled to dimensionless numbers by removing the dimensional parts, i.e.,  $l = \tilde{l}[\mu]$ ,  $\Lambda = \tilde{\Lambda}[\mu]$ , where  $[\mu]$  has unit magnitude carrying the dimension of momentum or mass dimension 1, while the  $\tilde{l}, \tilde{\Lambda}$  are dimensionless numbers. Now, we may change the integration variable from  $\tilde{l} \rightarrow \zeta$  as

$$\tilde{l} = \frac{\zeta}{(1-\zeta)^7}, \quad d\tilde{l} = d\zeta \frac{1+6\zeta}{(1-\zeta)^8}, \quad (\text{A8})$$

so that the integral equations are reduced to a coupled system of  $2N$  linear algebraic equations for  $i = 1, \dots, N$ :

$$\begin{bmatrix} t_a(p'_i, p; E) \\ t_b(p'_i, P; E) \end{bmatrix} = \sum_{j=1}^N \tilde{w}_j \frac{1+6\zeta_j}{(1-\zeta_j)^8} \times \begin{bmatrix} A(p'_i, \zeta_j) & B(p'_i, \zeta_j) \\ C(p'_i, \zeta_j) & D(p'_i, \zeta_j) \end{bmatrix} \begin{bmatrix} t_a(\zeta_j, p; E) \\ t_b(\zeta_j, p; E) \end{bmatrix}, \quad (\text{A9})$$

for a given initial center-of-mass kinetic energy  $E$ . The new Gaussian weights  $\tilde{w}_j$ , correspond to  $N$  intermediate points  $\zeta_j$  between the new integration limits  $[0, \lambda]$ , related to the previously defined ones by

$$w_j = \tilde{w}_j \frac{1+6\zeta_j}{(1-\zeta_j)^8}, \quad \tilde{\Lambda} = \frac{\lambda}{(1-\lambda)^7}. \quad (\text{A10})$$

After the integration, we restore the original form of the momentum cut-off from  $\lambda \rightarrow \Lambda$ . In this way we may expand the domain of numerical integration to include momenta up to 12 orders of magnitude, maintaining sufficient numerical accuracy.

The consistency of the above system of linear equations imply  $\det(X - I) = 0$ , the solution (zeros) to which determine the eigenenergies. As a demonstration, Fig. 12 displays the plot of  $\det(X - I)$  vs energy,  $-E = E_{D^0nn} > 0$ , for the  $D^0nn$  system for different sharp cut-offs.<sup>5</sup> The figure depicts the kinematic sector with  $E_{D^0nn}$  above the particle-dimer break-up threshold energy  $E_D \simeq 53.4$  MeV, as given by Eq. (55). Below  $E_D$  the three-body system energetically favors dissociating into a  $D^0n$  dimer and a neutron. The Efimov-like bound states emerge above this threshold which correspond to the zeros of the individual oscillatory curves.

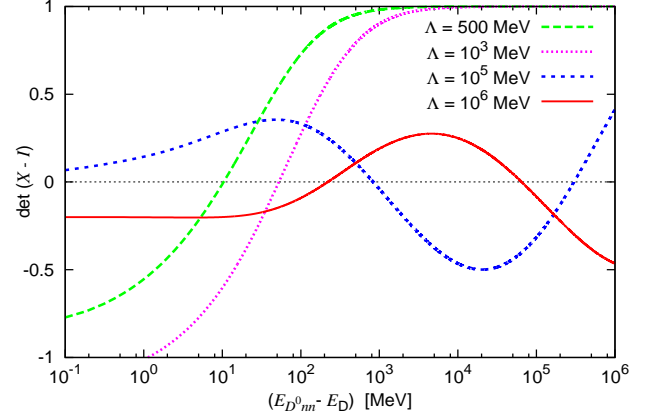


FIG. 12.  $\det(X - I)$  vs energy  $E_{D^0nn} - E_D$  plot for the  $D^0nn$  system for different sharp momentum cut-offs  $\Lambda$ .  $E_D \sim 53.4$  MeV is the threshold energy for break-up into a  $D^0n$  dimer and a neutron. The nodes (zeros) correspond to energy eigenvalues of Efimov-like level states.

### Appendix B: Convergence test of numerical integration

As a simple qualitative test of the asymptotic convergence of the limit cycle behavior, both due to cut-off dependent artifacts, as well as instabilities arising from the numerical integration, it may be instructive to investigate the behavior of the three-body parameter  $s_0 \equiv s_0^{(n)}$  in the non-asymptotic solution. Note the implicit dependence of this parameter on the  $n^{\text{th}}$  critical cut-off, indicated by the superscript  $n$ . Referring back to Fig. 10 in the main text, continuing to very large values of the cut-off  $\Lambda$ , a discrete sequence of critical points is obtained following a rough logarithmic periodicity  $\propto \pi/s_0^{(n)}$ . However, the crucial observation is that as  $\Lambda \rightarrow \infty$  this ratio must eventually converges to the *universal* value  $\pi/s_0^\infty$ , where  $s_0^\infty$  is a transcendental number characterizing the asymptotic limit cycle, irrespective of the values of inverse scattering lengths and energy eigenvalues of the bound state. In other words, if  $\Lambda_c^{(n)}$  and  $\Lambda_c^{(n+1)}$  are successive critical points corresponding to the  $n^{\text{th}}$  and  $(n+1)^{\text{th}}$  Efimov-like levels (with  $n = 0$  as the ground state) emerging at threshold then,

$$s_0^{(n)} = \frac{\pi}{\ln\left(\frac{\Lambda_c^{(n+1)}}{\Lambda_c^{(n)}}\right)}, \quad \lim_{n \rightarrow \infty} s_0^{(n)} = s_0^\infty. \quad (\text{B1})$$

This is exactly depicted in Fig. 13 for the case of the  $K^-nn$  bound Borromean state (left plot) and the  $D^0nn$  bound state (right plot), with fixed energy eigenvalue chosen sufficiently close to the respective thresholds. For the first few values of  $n$ , the ratios of the critical cut-offs display significant deviations due to finite cut-off effects. In fact, it is notable that the ground ( $n = 0$ ) state of three-body systems is predominantly known to display maximal deviations from universal features

<sup>5</sup> It is more clearly revealed in Fig. 10 (see main text), that the energy eigenvalues exist only for  $\Lambda \gtrsim 200$  MeV for this system.

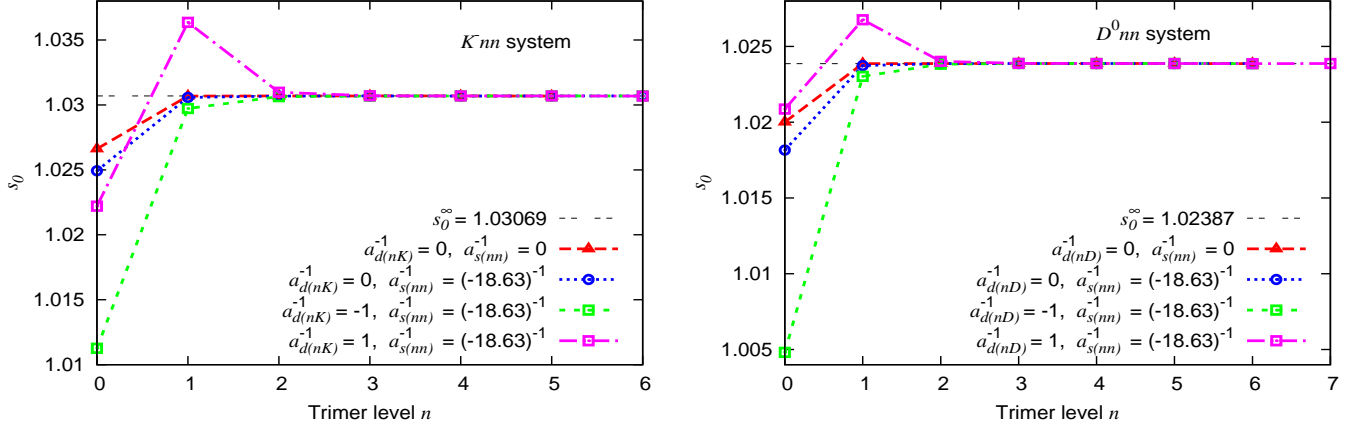


FIG. 13. Convergence of the three-body parameter  $s_0$  for a fixed energy eigenvalue close to respective thresholds for the  $K^-nn$  and  $D^0nn$  Efimov-like trimer states. The points corresponding to equal values of the two-body (inverse) scattering lengths (in  $\text{fm}^{-1}$ ) are connected by straight lines in order to guide the eyes. To achieve reasonable convergence up to the  $n = 7^{\text{th}}$  excited level state, the number of quadrature points used in the numerical integration is  $N = 300$ .

of the Efimov spectrum lying far beyond the universal window at around the unitary limit. However, both the plots suggest a rapid convergence of  $s_0$  towards the asymptotic values of  $s_0^\infty = 1.03069$  and  $1.02387$ , respectively, for  $n \geq 2$ . This is evidenced in all cases where different positive and negative values of the two-body (inverse) scattering lengths are chosen approaching the unitary limit from either directions, while the masses of mesons are kept fixed to the respective physical values. But despite this apparent convergence, beyond a certain number  $n$ , the numerical precision of the integration routine becomes poor, resulting in deviations again from the asymptotic values. In that case, numerical accuracy is systematically improved by an appropriate choice of the number of the quadrature points  $N$  somewhat large, e.g.,  $N \geq 300$  may be necessary to obtain reasonable convergence beyond the  $n = 7^{\text{th}}$  excited Efimov state in the above figure, where the corresponding critical cut-off exceeds beyond  $\Lambda_c^{(n>7)} \sim 10^{13}$  MeV. But the practical disadvantage of choosing a large  $N$  is the dramatic increase the computational time which is undesirable. However, in the context of our low-energy EFT analysis, the numerical integration is naturally restricted to low

cut-off values where an optimal choice, e.g.,  $N = 96$  yields reasonably good convergence up to the  $n = 5^{\text{th}}$  excited state through the additional reparameterization of the integration variable, as described in Appendix A.

## ACKNOWLEDGMENTS

The authors are grateful to Wolfram Weise for useful discussions. U.R. gratefully acknowledges the hospitality of YITP during the initial stages of the work. He also thanks G. Meher for using discussions. S.I.A. acknowledges the hospitality of IIT Guwahati during the final stage of the work. The work of Y.K. is supported in part by JSPS KAKENHI Grant Number JP17J04333. The work of S.I.A. is supported by the Basic Science Research Program through the National Research Foundation of Korea funded by the Ministry of Education of Korea (Grant No. NRF-2016R1D1A1B03930122). The work of T.H. is supported in part by JSPS KAKENHI Grant Number JP16K17694 and by the Yukawa International Program for Quark-Hadron Sciences (YIPQS).

- 
- [1] T. Hyodo and D. Jido, Prog. Part. Nucl. Phys. **67**, 55 (2012).
  - [2] A. Gal, E. V. Hungerford and D. J. Millener, Rev. Mod. Phys. **88**, 035004 (2016).
  - [3] Y. Nogami, Phys. Lett. **7**, 288 (1963).
  - [4] Y. Akaishi and T. Yamazaki, Phys. Rev. C **65**, 044005 (2002).
  - [5] N. V. Shevchenko, A. Gal and J. Mares, Phys. Rev. Lett. **98**, 082301 (2007).
  - [6] N. V. Shevchenko, A. Gal, J. Mares and J. Revai, Phys. Rev. C **76**, 044004 (2007).
  - [7] Y. Ikeda and T. Sato, Phys. Rev. C **76**, 035203 (2007).
  - [8] Y. Ikeda and T. Sato, Phys. Rev. C **79**, 035201 (2009).
  - [9] T. Yamazaki and Y. Akaishi, Phys. Rev. C **76**, 045201 (2007).
  - [10] A. Dote, T. Hyodo and W. Weise, Nucl. Phys. A **804**, 197 (2008).
  - [11] A. Dote, T. Hyodo and W. Weise, Phys. Rev. C **79**, 014003 (2009).
  - [12] S. Wycech and A. Green, Phys. Rev. C **79**, 014001 (2009).

- [13] Y. Ikeda, H. Kamano and T. Sato, *Prog. Theor. Phys.* **124**, 533 (2010).
- [14] N. Barnea, A. Gal and E. Liverts, *Phys. Lett. B* **712**, 132 (2012).
- [15] S. Ohnishi, W. Horiuchi, T. Hoshino, K. Miyahara and T. Hyodo, *Phys. Rev. C* **95**, 065202 (2017).
- [16] J. Revai, *Phys. Rev. C* **94**, 054001 (2016)
- [17] T. Hoshino, S. Ohnishi, W. Horiuchi, T. Hyodo and W. Weise, arXiv:1705.06857 [nucl-th].
- [18] T. Uchino, T. Hyodo and M. Oka, *Nucl. Phys. A* **868-869**, 53 (2011).
- [19] A. Hosaka, T. Hyodo, K. Sudoh, Y. Yamaguchi and S. Yasui, *Prog. Part. Nucl. Phys.* **96**, 88 (2017).
- [20] N. Brambilla *et al.*, *Eur. Phys. J. C* **71**, 1534 (2011).
- [21] A. Hosaka, T. Iijima, K. Miyabayashi, Y. Sakai and S. Yasui, *PTEP* **2016**, 062C01 (2016).
- [22] C. Patrignani, *Chin. Phys. C* **40**, 100001 (2016).
- [23] J. Hofmann and M. F. M. Lutz, *Nucl. Phys. A* **763**, 90 (2005).
- [24] T. Mizutani and A. Ramos, *Phys. Rev. C* **74**, 065201 (2006).
- [25] C. Garcia-Recio *et al.*, *Phys. Rev. D* **79**, 054004 (2009).
- [26] J. Haidenbauer, G. Krein, U.-G. Meissner and L. Tolos, *Eur. Phys. J. A* **47**, 18 (2011).
- [27] Y. Yamaguchi, S. Ohkoda, S. Yasui and A. Hosaka, *Phys. Rev. D* **84**, 014032 (2011).
- [28] Y. Yamaguchi, S. Ohkoda, S. Yasui and A. Hosaka, *Phys. Rev. D* **87**, 074019 (2013).
- [29] M. Bayar *et al.*, *Phys. Rev. C* **86**, 044004 (2012).
- [30] Y. Yamaguchi, S. Yasui and A. Hosaka, *Nucl. Phys. A* **927**, 110 (2014).
- [31] E. Braaten and H.-W. Hammer, *Phys. Rept.* **428**, 259 (2006).
- [32] P. Naidon and S. Endo, *Rept. Prog. Phys.* **80**, 056001 (2017).
- [33] V. Efimov, *Phys. Lett. B* **33**, 563 (1970).
- [34] E. Braaten and H. Hammer, *Phys. Rev. Lett.* **91**, 102002 (2003).
- [35] E. Braaten and M. Kusunoki, *Phys. Rev. D* **69**, 074005 (2004).
- [36] T. Hyodo, T. Hatsuda and Y. Nishida, *Phys. Rev. C* **89**, 032201 (2014).
- [37] S.-I. Ando, U. Raha and Y. Oh, *Phys. Rev. C* **92**, 024325 (2015).
- [38] SIDDHARTA Collaboration, M. Bazzi *et al.*, *Phys. Lett. B* **704**, 113 (2011).
- [39] SIDDHARTA Collaboration, M. Bazzi *et al.*, *Nucl. Phys. A* **881**, 88 (2012).
- [40] U. G. Meissner, U. Raha and A. Rusetsky, *Eur. Phys. J. C* **35**, 349 (2004).
- [41] Y. Ikeda, T. Hyodo and W. Weise, *Phys. Lett. B* **706**, 63 (2011).
- [42] Y. Ikeda, T. Hyodo and W. Weise, *Nucl. Phys. A* **881**, 98 (2012).
- [43] Y. Yamaguchi and T. Hyodo, *Phys. Rev. C* **94**, 065207 (2016).
- [44] N. Kaiser, P. B. Siegel and W. Weise, *Nucl. Phys. A* **594**, 325 (1995).
- [45] E. Oset and A. Ramos, *Nucl. Phys. A* **635**, 99 (1998).
- [46] J. A. Oller and U. G. Meissner, *Phys. Lett. B* **500**, 263 (2001).
- [47] T. Hyodo, D. Jido and A. Hosaka, *Phys. Rev. C* **78**, 025203 (2008).
- [48] R. Eden and J. Taylor, *Phys. Rev.* **133**, B1575 (1964).
- [49] B. C. Pearce and B. F. Gibson, *Phys. Rev. C* **40**, 902 (1989).
- [50] A. Cieply, M. Mai, U.-G. Meissner and J. Smejkal, *Nucl. Phys. A* **954**, 17 (2016).
- [51] T. Hyodo, *Phys. Rev. C* **90**, 055208 (2014).
- [52] H. W. Hammer, *Nucl. Phys. A* **705**, 173 (2002).
- [53] S.-I. Ando and M. C. Birse, *J. Phys. G* **37**, 105108 (2010).
- [54] S.-I. Ando, G.-S. Yang, and Y. Oh, *Phys. Rev. C* **89**, 014318 (2014).
- [55] S.-I. Ando and Y. Oh, *Phys. Rev. C* **90**, 037301 (2014).
- [56] H. W. Hammer, C. Ji, and D. R. Phillips, arXiv:1702.08605 [nucl-th].
- [57] D. B. Kaplan, M. J. Savage and M. B. Wise, *Phys. Lett. B* **424**, 390 (1998).
- [58] D. B. Kaplan, M. J. Savage and M. B. Wise, *Nucl. Phys. B* **534**, 329 (1998).
- [59] S. R. Beane and M. J. Savage, *Nucl. Phys. A* **694**, 511 (2001).
- [60] S.-I. Ando and C. H. Hyun, *Phys. Rev. C* **72**, 014008 (2005).
- [61] P. F. Bedaque, H. W. Hammer, and U. van Kolck, *Nucl. Phys. A* **646**, 444 (1999).
- [62] G. S. Danilov and V. I. Lebedev, *Sov. Phys. JETP* **17** (1963) 1015.
- [63] Q. Chen *et al.*, *Phys. Rev. C* **77**, (2008), 054002-1.
- [64] L. H. Thomas, *Phys. Rev.* **47**, 903 (1935).